

# Gamma production cross sections from 14-MeV neutron bombardment of $^{89}\text{Y}^\dagger$

F. S. Dietrich, M. C. Gregory,\* and J. D. Anderson  
Lawrence Livermore Laboratory, Livermore, California 94550

(Received 5 October 1973)

$\gamma$  decays of levels in  $^{88}\text{Y}$  and  $^{89}\text{Y}$  have been observed with a Ge(Li) spectrometer following 14.1-MeV neutron bombardment of natural yttrium metal. Prompt and delayed ( $> 50$  nsec) radiations were separated by pulsing the neutron source. Following the reaction  $^{89}\text{Y}(n, 2n)^{88}\text{Y}$ , delayed  $\gamma$  rays of 442 and 232 keV are ascribed to the decay sequence  $8^+$  (674 keV)  $\rightarrow 5^-$  (232)  $\rightarrow 4^-$  (0) and a 393-keV  $\gamma$  ray to the transition  $1^+$  (393)  $\rightarrow 4^-$  (0). A delayed 909-keV radiation corresponds to the decay of the first excited state of  $^{89}\text{Y}$ . Cross sections were determined with an uncertainty of  $\pm 11\%$  for the delayed radiations and  $\pm 30\%$  for the remainder. A statistical-model calculation for the  $^{89}\text{Y}(n, 2n)^{88}\text{Y}$  reaction reproduces the observed cross sections only if the  $\gamma$  branching ratios in  $^{88}\text{Y}$  are taken from experiment, and in particular, the  $(g_{9/2})^2$  multiplet is included.

NUCLEAR REACTIONS  $^{89}\text{Y}(n, 2n\gamma)^{88}\text{Y}$ ,  $^{89}\text{Y}(n, n'\gamma)^{89}\text{Y}$ .  $E = 14.1$  MeV; measured  $E_\gamma$ ,  $\sigma(E_\gamma)$ . Deduced  $\sigma(E_\gamma)$  dependence on  $J, \pi$  in  $^{88}\text{Y}$ . Natural target, Ge(Li) detector.

## I. INTRODUCTION

The purpose of the present work is to investigate the prompt and delayed  $\gamma$ -radiation following bombardment of  $^{89}\text{Y}$  with 14-MeV neutrons, and to relate the observed cross sections to the structure of  $^{88}\text{Y}$  and  $^{89}\text{Y}$ . At the time of the most recent survey of  $A = 88$  nuclei,<sup>1</sup> only five excited states of  $^{88}\text{Y}$  had been assigned reasonably probable spins and parities; since then, much additional spectroscopic information has been reported which is necessary to explain the results of the present experiment.

Two isomers have been established in  $^{88}\text{Y}$ . The lower-lying isomer, which was first observed by Hyde, Florence, and Larsh<sup>2</sup> following electron capture in  $^{88}\text{Zr}$ , connects the  $1^+$  second excited state of  $^{88}\text{Y}$  at 393 keV with the  $4^-$  ground state. The half-life for this transition adopted by Ref. 1 is 0.30 msec. A second isomer having a half-life<sup>1</sup> of 13.6 msec, which appears to have been first observed<sup>3</sup> by 20-MeV proton bombardment of  $^{89}\text{Y}$ , yields two  $\gamma$ -rays of energies near 230 and 450 keV,<sup>4,5</sup> of roughly equal intensities. In the mid-stream evaluation,<sup>1</sup> Goodman *et al.* have assigned the  $\gamma$  rays to the cascade 687 keV( $8^+$ )  $\rightarrow$  231( $5^-$ )  $\rightarrow$  0( $4^-$ ).

At Argonne,<sup>6</sup> a series of charged-particle reactions has been used to locate at least 29 states below 2.5 MeV excitation in  $^{88}\text{Y}$ . Spin-parity assignments and spectroscopic configurations were suggested for most of the levels observed below 1.5 MeV. An important feature of the spectrum

which bears strongly on the present work is a  $(g_{9/2})_p(g_{9/2})_n^{-1}$  multiplet, closely resembling the multiplet observed by the same group<sup>7</sup> in  $^{90}\text{Nb}$ . The 687-keV isomeric state presumably corresponds to the lowest-lying ( $8^+$ ) member of this multiplet. Baer *et al.*<sup>8</sup> have observed  $\gamma$  transitions in  $^{88}\text{Y}$  following the  $^{85}\text{Rb}(\alpha, n\gamma)$  reaction; they determined the energies of the  $\gamma$  rays with high precision ( $\lesssim \frac{1}{2}$  keV), and fitted nearly all of the observed transitions into the level scheme suggested by the Argonne experiments.  $\gamma$  decay of states in  $^{88}\text{Y}$  has also been observed following excitation by the  $^{88}\text{Sr}(p, n)^{88}\text{Y}$  reaction.<sup>9</sup>

In the present experiment, the use of a Ge(Li) spectrometer allowed sufficient resolution to identify prompt radiation in the presence of neutron-induced background, as well as delayed radiation. The precision of the energy calibration allowed identification of  $\gamma$  rays common to the  $^{89}\text{Y}(n, 2n)^{88}\text{Y}$  reaction and the  $^{85}\text{Rb}(\alpha, n\gamma)^{88}\text{Y}$  reaction of Ref. 8. We have calculated the  $\gamma$  production cross sections using a statistical (Hauser-Feshbach) model for the reaction sequence  $^{89}\text{Y}(n, n')^{89}\text{Y}(n)^{88}\text{Y}$ . Because the  $^{89}\text{Y}(n, 2n)$  reaction  $Q$  of  $-11.48$  MeV allows  $^{88}\text{Y}$  excitation energies only up to about 2.6 MeV, details of the  $\gamma$  cascade in the final nucleus were taken from experiment rather than from a statistical model. The calculation successfully reproduces the experimental results only if the strong transitions observed between members of the  $g_{9/2}^2$  multiplet are taken into account. In particular, the population of the  $8^+$  level is dominated by  $\gamma$  decays from higher-lying  $6^+$  and  $7^+$

levels.

## II. EXPERIMENTAL METHODS AND RESULTS

The 14-MeV neutrons were supplied by the Livermore ICT (insulated-core transformer) neutron generator. The experimental geometry is shown in Fig. 1. Deuterons of 400-keV energy and currents up to 20  $\mu\text{A}$  impinged on a solid tritium-titanium target. The deuterons passed through a capacitive pickup cylinder, which provided a time reference signal for the portions of the experiment in which the beam was pulsed. Neutron production was monitored by counting  $\alpha$  particles from the  ${}^3\text{H}(d, n){}^4\text{He}$  reaction in a silicon surface-barrier counter at  $174^\circ$  to the incident deuteron beam. The absolute neutron source strength was determined by comparing the  $\alpha$  counting rate with the counting rate in a calibrated NE213 liquid scintillator whose efficiency is believed to be known to  $\pm 7\%$ . The neutron production rate was typically  $10^9 \text{ sec}^{-1}$ . The yttrium target was a ring of natural (monoisotopic) metal, having outside diameter 17.8 cm, inside diameter 12.7 cm, thickness 1.27 cm, and weighing 679.6 g.

$\gamma$  rays were counted by a Ge(Li) detector of 7.8-cm<sup>3</sup> nominal active volume placed 1 to 1.5 m from the yttrium sample. The resolution for 511-keV  $\gamma$  rays was approximately 5 keV. Background induced by room-scattered neutrons was reduced by a 10.2-cm wall of lead bricks around the detector. Neutrons coming directly from the source were attenuated by a copper shadow cone 45.7 cm long and 7.6 cm in diameter at its widest point. The yttrium ring was mounted with its axis along the line from the neutron source to the detector, and with the source near the center of the ring; the incident deuteron beam struck the target at an angle of  $30^\circ$  with respect to the ring axis. In this geometry, the average energy of neutrons striking the ring was 14.1 MeV, with a

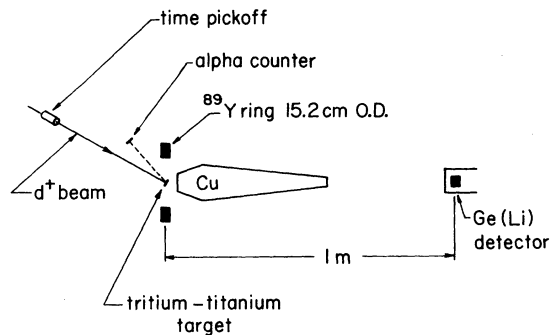


FIG. 1. Geometry for  ${}^{89}\text{Y} + n$  experiment.

spread of approximately  $\pm 300$  keV.

The prompt and delayed components of the radiation were identified by pulsing the beam and timing the detected  $\gamma$  rays with respect to the pulses. Two series of runs were made. In the first, the beam was pulsed at a rate of 2.5 MHz, and in the second at 0.5 MHz. The pulse widths were less than 10 nsec, which allowed timing windows of about 20 nsec to be set for the prompt radiation. In both series, the time between pulses was short compared to the half-lives of the expected isomeric transitions, which were 300  $\mu\text{sec}$  and 13.4 msec in  ${}^{88}\text{Y}$ , and 16 sec in  ${}^{89}\text{Y}$ . Delayed radiation was examined by setting a wide timing window just earlier than the prompt radiation, but late enough after the preceding beam pulse to avoid most fast-neutron-induced reactions in the detector. Spectra with an unpulsed beam were recorded in each case, with and without the yttrium sample present.

Examples of the spectra collected during the second series of runs are shown in Fig. 2. The top spectrum was taken without time gating. The middle and bottom spectra were taken with prompt and delayed time gates, respectively. The three spectra were collected in two hours each; counting rates were in the range of 2000 to 5000  $\text{sec}^{-1}$ . The time gates were approximately 40 nsec and 600 nsec for the prompt and delayed spectra, respectively. The peaks up to 910 keV due to reactions in the yttrium sample are indicated in Fig. 2, and are listed in the first column of Table I, together with five additional peaks up to about 1500 keV.

TABLE I.  $\gamma$  rays observed in  ${}^{89}\text{Y} + n$  reactions. Cross sections have uncertainties  $\pm 11\%$  for values above 100 mb, and  $\pm 30\%$  below. Cross sections for the prompt  $\gamma$  rays are to be interpreted as  $4\pi(d\sigma/d\Omega)_{90^\circ}$ . Energy uncertainties  $\pm 0.5$  keV below 1000 keV;  $\pm 1.5$  keV above.

$E$ (keV)	$\sigma$ (mb)	${}^{85}\text{Rb}(\alpha, n)$ (Ref. 8)	${}^{88}\text{Sr}(p, n)$ (Ref. 9)	Prompt	Delayed	${}^{89}\text{Y}$	Not placed
127.6	34	x		x			
141.4	17	x	x	x			
231.6	403	x	x	x	x		
298.7	11	x	x	x			
313.5	33	x	x	x			
373.5	17	x	x	x			
392.7	114	x	x		x		
442.4	136	x			x		
(537.7)	17			x			x
611.4	11	x	x	x			
(715.7)	13		x	x			x
776.9	29			x			x
897.2	53	x		x			(x)
909.1	439				x	x	
(962.0)	17			x			x
984.3	40	x	x	x			
1087.8	25	x	x	x			
1311.0	42			x			x
1506.4	54			x			x

Doubtful assignments are placed in parentheses in the table. The remaining peaks were seen either in spectra with the sample removed or in spectra with the beam off. Delayed radiations were found only at 232, 393, 442, and 909 keV; the 232-keV  $\gamma$  ray has both prompt and delayed components. An activation  $\gamma$  ray partially obscures the 141-keV  $\gamma$  ray in the ungated spectrum, but the activation component is negligible in the prompt spectrum.

The energy calibration for the peaks was made by taking a spectrum without time gating and with several calibration sources from 122 to 1332 keV present. A least-squares fit of a cubic polynomial to the calibration lines was made, and the resulting coefficients used to determine the energies of the lines at 127.6, 231.6, 313.5, 392.7, 442.4, and

909.1 keV. These energies and the 511-keV annihilation radiation were then used to determine the energies of the remaining lines in Fig. 2 and Table I by a similar cubic fit. The uncertainties in the energies are estimated as  $\pm 0.5$  keV for  $\gamma$ -ray energies below 1000 keV and  $\pm 1.5$  keV above 1000 keV.

The cross sections for production of the  $\gamma$  rays associated with the sample are listed in Table I. Cross sections for most of the  $\gamma$  rays, including the 232-, 392-, 442-, and 909-keV radiations, were taken from the ungated spectra. Then the cross sections for a few of the weakly excited  $\gamma$  rays were found from the prompt-gated spectra by normalizing their intensities to those already determined for the strong radiations. Efficiency

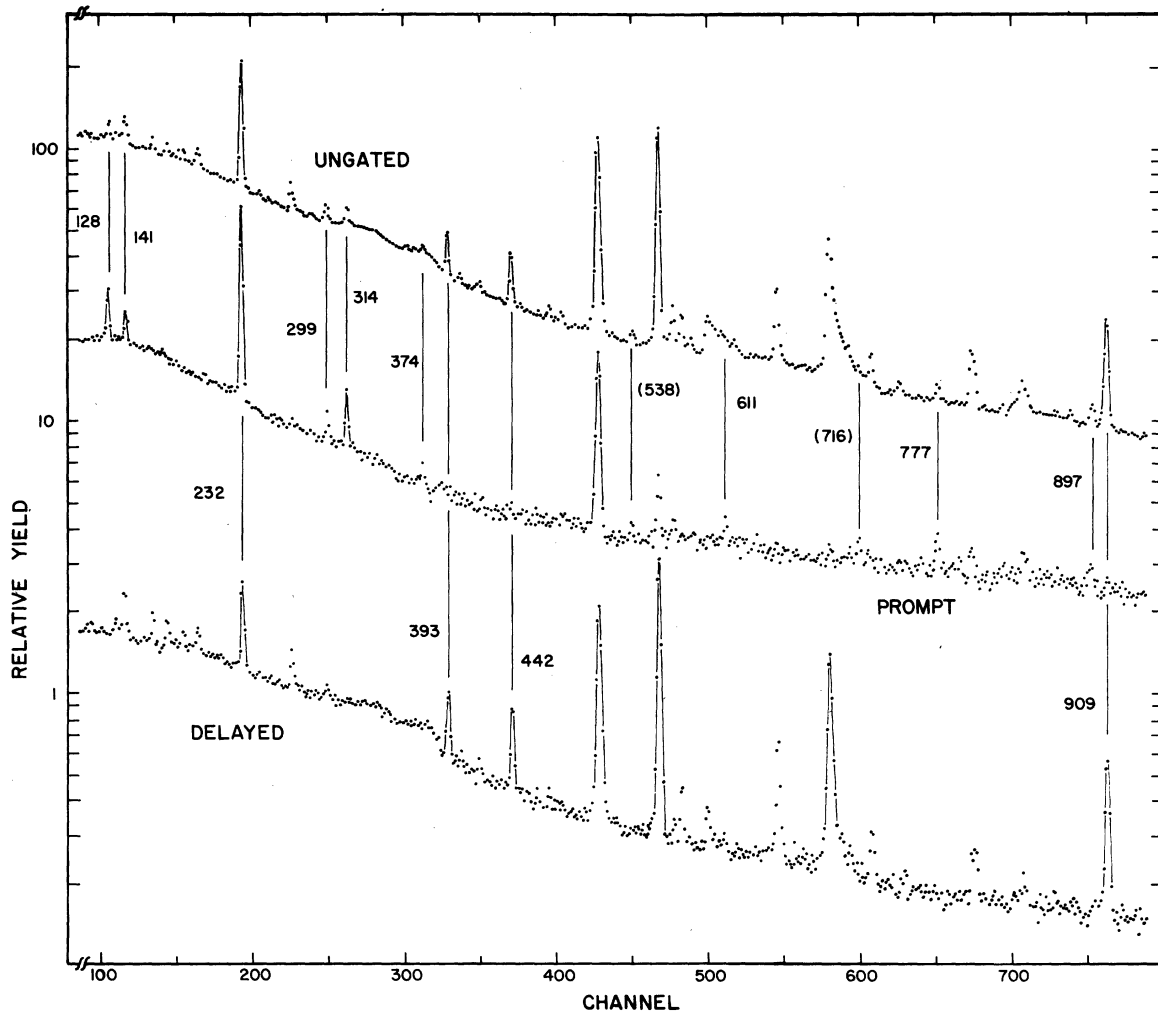


FIG. 2. A portion of the pulse-height spectrum. Upper spectrum: unpulsed beam; middle spectrum: pulsed beam, gate open for prompt  $\gamma$  events; lower spectrum: gated for delayed events. The vertical positions of the three spectra are arbitrary.

calibration of the detector was accomplished with a set of International Atomic Energy Agency calibrated sources<sup>10</sup> (<sup>57</sup>Co, <sup>203</sup>Hg, <sup>22</sup>Na, <sup>137</sup>Cs, <sup>54</sup>Mn, <sup>60</sup>Co, <sup>88</sup>Y). The sources were placed on the yttrium ring during the calibration. The uncertainty in the efficiency determination is estimated as  $\pm 7\%$ . Corrections for self-absorption of the  $\gamma$  rays in the yttrium sample were determined from the tables of Storm and Israel<sup>11</sup> and were in the range of 35 to 15% from 232 to 909 keV. The neutron flux, which had an estimated uncertainty of  $\pm 7\%$ , required a small correction for self-absorption in the yttrium sample. This correction was estimated at 6% with a contribution to the error in the final results of  $\pm 2\%$ .

The error in extracting the counts in the peaks in the ungated runs for the strongest transitions at 232, 393, 442, and 909 keV was estimated as  $\pm 5\%$ . The combined error in the absolute cross sections for these  $\gamma$  rays is  $\pm 11\%$ . For each of these  $\gamma$  rays, the cross sections from the two independent determinations agreed to better than  $\pm 7\%$ . The average of the two sets is shown in Table I. The 442-keV  $\gamma$  ray and the delayed component of the 232-keV  $\gamma$  ray agreed in intensity to better than 10%. For the remaining transitions, the uncertainty is estimated as  $\pm 30\%$ . We have assumed throughout that the angular distributions are isotropic, which is reasonable for the delayed radiations, since their half-lives are long compared to thermal relaxation times for the spins. A comparison of the present isomeric cross sections with previously reported values<sup>12-16</sup> is shown in Table II. Agreement with the results of Broadhead, Shanks, and Heady<sup>16</sup> is good for the 909-keV transition in <sup>89</sup>Y. Our measurement for the 393-keV transition in <sup>88</sup>Y is consistent with the recent value of Salaita and Eapen,<sup>13</sup> but for the 442-keV transition is more than 30% smaller than their value. The 700-keV difference in incident

neutron energy may possibly account for the discrepancy.

In Table I we have attempted to assign the  $\gamma$  transitions to the various accessible nuclei. All except those indicated in the last two columns have been assigned to <sup>88</sup>Y by comparison with the results of the Colorado group<sup>8</sup> from the reaction <sup>85</sup>Rb( $\alpha, n\gamma$ ). The energies found in the present experiment agree with those of Ref. 8 to better than 0.5 keV except for the 984-keV  $\gamma$  ray, which differs by 0.8 keV. The assignments of four  $\gamma$  rays to <sup>89</sup>Y, including the 909-keV isomeric transition, are based on comparison with the results of Buchanan *et al.*<sup>17</sup> on the <sup>89</sup>Y( $n, n'\gamma$ ) reaction at energies well below the ( $n, 2n$ ) threshold. The 897-keV  $\gamma$  ray cannot be assigned conclusively to <sup>88</sup>Y even though it was seen in the <sup>85</sup>Rb( $\alpha, x\gamma$ ) experiment, since it may be the decay of the 2.734-MeV level in <sup>88</sup>Sr following the <sup>89</sup>Y( $n, d$ )<sup>88</sup>Sr reaction in the present experiment or <sup>85</sup>Rb( $\alpha, p$ ) in the Colorado experiment. However, the measured centroid energy of 897.2 keV is sufficiently less than the 898.04-keV energy<sup>18</sup> of the transition in <sup>88</sup>Sr to favor assignment of this  $\gamma$  ray to <sup>88</sup>Y. The  $\gamma$  rays at 538, 777, and 962 keV remain unplaced.

We have fitted the  $\gamma$  rays ascribed to <sup>88</sup>Y into the level sequence shown in Fig. 3, using the level schemes of the Argonne<sup>6</sup> and Colorado<sup>8</sup> experiments for guidance. The spin-parity assignments are the ones suggested by the Argonne group, except for the 706-keV level, which was not observed in their work. The midstream evaluation<sup>1</sup> has assigned  $1^+$  for this level. However, Dutt and Gabbard<sup>19</sup> and Gabbard, Chenevert, and Sekharan<sup>9</sup> have proposed  $2^-$  assignments. Most recently, Daehnick and Bhatia<sup>20</sup> have presented evidence for a positive-parity assignment of low spin ( $1^+, 2^+$ ) and have suggested the possibility of a doublet. Any of these assignments are consistent with a dominant transition to the  $1^+$  (393-keV) level.

TABLE II. Measured isomeric cross sections from <sup>89</sup>Y +  $n$  near  $E_n = 14$  MeV.

Transition (keV)	Present <sup>a</sup> (mb)	Other measurements
393 ( $1^+ \rightarrow 4^-$ )	114 $\pm$ 13	100 <sup>b</sup> Monnard (Ref. 12), 14.3 MeV 96 $\pm$ 8 Salaita and Eapen (Ref. 13), 14.8 MeV
442 ( $8^+ \rightarrow 5^-$ )	136 $\pm$ 15	>400 Glagolev and Yampol'skii (Ref. 14), 14.7 MeV 150 <sup>b</sup> Monnard (Ref. 12), 14.3 MeV 74 $\pm$ 25 Van Zelst, Meyers, and Oosting (Ref. 15), nom, 14 MeV 227 $\pm$ 18 Salaita and Eapen (Ref. 13), 14.8 MeV
909 ( $\frac{3}{2}^+ \rightarrow \frac{1}{2}^-$ )	439 $\pm$ 48	400 $\pm$ 47 Broadhead, Shanks, and Heady (Ref. 16), 14.6 MeV

<sup>a</sup> Neutron energy 14.1  $\pm$  0.3 MeV.

<sup>b</sup> No uncertainties quoted.

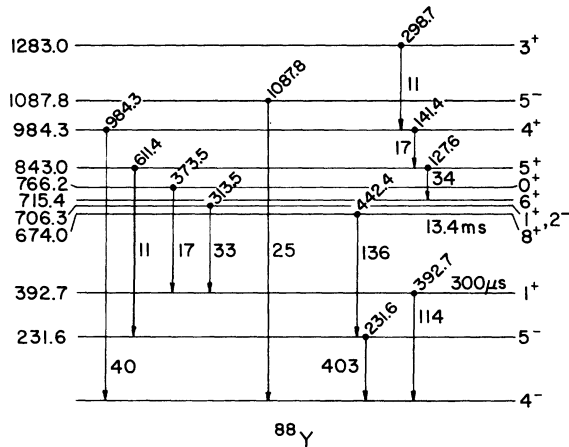


FIG. 3.  $\gamma$  rays identified in  $^{88}\text{Y}$  in the present experiment. The  $\gamma$  transitions are labeled with their energies and their production cross sections.

### III. CALCULATION OF LEVEL POPULATIONS IN $^{88}\text{Y}$

The cross sections for population of states in  $^{88}\text{Y}$  by the  $^{89}\text{Y}(n, 2n)$  reaction were calculated by assuming a compound-nucleus reaction sequence and computing the populations at each stage by the Hauser-Feshbach method.<sup>21</sup> In this section the calculation is described, and it is shown that the populations of the various levels in  $^{88}\text{Y}$  are insensitive to variations in the parameters of the theory. The succeeding  $\gamma$  decay of levels in  $^{88}\text{Y}$  is discussed in the next section, and it is found that the  $\gamma$ -production cross sections for the low-lying levels can be reproduced.

Figure 4 shows the reaction sequence. In the first stage, the cross section for formation of the compound nucleus  $^{90}\text{Y}^*$  is calculated for each spin and parity. The transmission coefficients  $T_{i,j}$  were calculated with the optical-model computer program LOKI using the Bjorklund-Fernbach optical potential<sup>22</sup> for incident neutrons of energy 14.7 MeV(lab). This energy is somewhat higher than the mean energy of 14.1 MeV in the present experiment, and almost as high as the 14.8 MeV in that of Ref. 13. The cross sections are largest near spins 4 and 5, and fall to half maximum near spins 2 and 7. The sum of the calculated partial absorption cross sections is 1600 mb.

In the next stage, the compound nucleus decays to highly excited states of  $^{89}\text{Y}$ , described by an energy- and spin-dependent level-density function given by the conventional constant temperature form

$$\rho(J, E) \propto (2J+1) \exp[-J(J+1)/2\sigma^2] \exp(E/T).$$

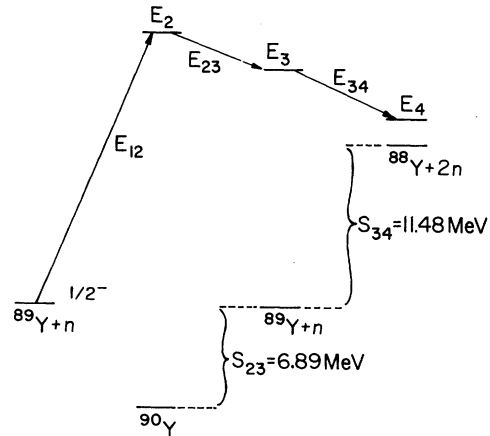


FIG. 4. Reaction scheme for the statistical model calculation of the  $^{88}\text{Y}(n, 2n)$  cross sections.

Black-nucleus transmission coefficients were used for this stage. The final results for the  $\gamma$  intensities are insensitive to the form of the transmission coefficients and to reasonable variations in the spin-cutoff parameter  $\sigma$  and the temperature  $T$ , as will be discussed below. The values adopted in this calculation are  $T=0.7$  MeV and  $\sigma=3.3$ , which are derived from neutron spectra in the reaction  $^{93}\text{Nb}(\alpha, n)^{96}\text{Tc}$  at  $E_\alpha=16$  MeV.<sup>23</sup>

In the final stage of the reaction, states in  $^{89}\text{Y}$  above the neutron emission threshold decay to  $^{88}\text{Y}$ . Since the maximum available excitation energy in  $^{88}\text{Y}$  is less than 3 MeV, a statistical distribution of its levels is inappropriate, and we use the experimentally determined level scheme. The transmission coefficients for this stage were derived from Moldauer's potential.<sup>24</sup>

No mechanism has been included in the calculation to account for the observed strong population of low-lying states in  $^{89}\text{Y}$  at 909, 1311, and 1506 keV. It would be possible to force the calculation to populate levels in  $^{89}\text{Y}$  below the neutron emission threshold by altering the form of the level-density function or the temperature. However, these states may also be formed by preequilibrium emission<sup>25</sup> from  $^{90}\text{Y}^*$ , and by direct reactions, possibly followed by a  $\gamma$  cascade. Since these mechanisms are not included in our calculation, we have normalized the sum of calculated cross sections in  $^{88}\text{Y}$  to 975 mb. This value represents a rough average of the measured  $^{89}\text{Y}(n, 2n)$ - $^{88}\text{Y}$  cross sections,<sup>13,26,27</sup> which show considerable spread. Charged-particle emission channels have been neglected throughout, as they presumably contribute little (<10%) to the decays.

The results of the calculation are presented in Table III for three choices of levels in  $^{88}\text{Y}$ . Selec-

tion I includes nearly all of the levels in  $^{88}\text{Y}$  for which spin-parity assignments have been suggested. It is to be emphasized that some of the assignments, particularly for the levels above 1 MeV, may be in error. Selection II includes only those levels connected by transitions identified in the present experiment, plus a presumed  $7^+$  level near 715 keV, originally suggested by the Argonne experiments,<sup>8</sup> which is necessary to explain the observed  $\gamma$  intensities. Selection III includes only the lowest four levels.

The sensitivity to the parameters of the model will be discussed for selection II, which is most applicable to the results of the present experiment. If the Moldauer potential is used for the transmission coefficients for  $^{89}\text{Y}-^{88}\text{Y}$ , the final populations change less than 5%. There is a substantial difference in the Moldauer and black-nucleus transmission coefficients, since the Moldauer potential yields the minimum in the  $s$ -wave and maximum in the  $p$ -wave strength functions in the region around  $A=100$ . Using black-nucleus coefficients for both decay stages changes the results by amounts less than 15%. Decreasing the temperature by 10% produces changes up to 4%.

The dependence of the populations on the spin cutoff parameter in  $^{89}\text{Y}$  is shown in Fig. 5. Values of  $\sigma$  between 3.0 and 4.25 correspond to moments of inertia between one-half rigid sphere and full rigid sphere, respectively; the measured values for neighboring nuclei fall within this region.<sup>28</sup> With the exception of the  $8^+$  level, the calculated cross sections vary only 20% or less within the

range of half to full rigid sphere. Although the  $8^+$  population cross section varies by 35% in this interval, we shall see that the observed  $\gamma$  decay rate is dominated by cascades to the level, and hence is insensitive to the variation.

#### IV. DISCUSSION

The usual methods for relating isomeric  $\gamma$  cross sections to the initial populations are based on the work of Huizenga and Vandebosch,<sup>29,30</sup> in which a cascade of dipole transitions is assumed to occur from the high-lying initial levels to the low-lying isomeric levels. The intermediate states in the cascade are described by a statistical spin distribution similar to that used for  $^{89}\text{Y}^*$  in the preceding section. The populations of the low-lying levels are then dependent on the spins of the levels, the spin-cutoff parameter, and the number of steps in the cascade. Such a treatment is not applicable in the present case because the maximum  $^{88}\text{Y}$  excitation energy of about 2.6 MeV is too low for a statistical distribution of the levels to be appropriate. In the simple statistical calculation the final level populations are determined by the distribution of spins immediately preceding the last  $\gamma$  decays according to a prescription requiring minimum spin change. For the present case we are interested in the distribution of cross section among the  $1^+$  and  $8^+$  isomers and the lowest  $4^-$  and  $5^-$  states. Then we should expect the  $8^+$  to be populated from states of spin 7 or greater, whereas the  $4^-$  and  $5^-$  should be populated from levels of spins 3 to 6. However,

TABLE III. Cross sections in mb for  $^{88}\text{Y}(n, 2n)^{88}\text{Y}$  calculated according to the Hauser-Feshbach model described in the text.

$E_x$ (keV)	$J^\pi$	I	II	III
0	$4^-$	203	253	370
232	$5^-$	136	181	287
393	$1^+$	58	74	199
674	$8^+$	32	37	117
706	$1^+$	40	55	
715	$6^+$	64	75	
715	$7^+$	48	54	
766	$0^+$	12	17	
843	$5^+$	70	84	
984	$4^+$	66	83	
1129	$5^-$	59		
1283	$3^+$	44	61	
1221	$1^+$	23		
1321	$5^-$	48		
1477	$9^+$	7		
1574	$2^+$	25		
1703	$3^+$	26		
2056	$2^+$	12		

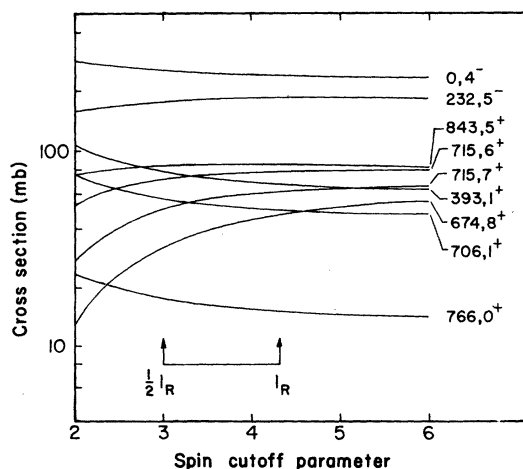


FIG. 5. Cross sections for population of levels in  $^{88}\text{Y}$  from the  $^{88}\text{Y}(n, 2n)$  reaction, computed as a function of the spin-cutoff parameter according to the statistical model calculation of Sec. III. The moment-of-inertia values corresponding to one-half and full rigid sphere are indicated.

this conclusion is strongly altered by the spectroscopic configurations of the low-lying levels.

The  $3^+$ ,  $4^+$ ,  $5^+$ ,  $6^+$ , and  $8^+$  levels shown in Fig. 3 are presumed to be members of the particle-hole multiplet formed from the configuration  $(g_{9/2})_{\text{proton}} \times (g_{9/2}^{-1})_{\text{neutron}}$ . The  $7^+$  member is believed<sup>6</sup> to lie within 15 keV of the  $6^+$ . Adjacent members of the multiplet are connected by strong  $M1$  transitions which are of the order of a full single-particle unit. In the experiment this can be seen in the transitions between the  $3^+$ ,  $4^+$ ,  $5^+$ , and  $6^+$  levels, which compete with  $E1$  decays to the lowest  $4^-$  and  $5^-$  states. No decay of the  $6^+$  level was observed in the present experiment; an upper limit of 5 mb may be placed on the 483-keV transition to the  $5^-$  first excited state. The observation of 34 mb feeding the state from higher levels plus the additional neutron feeding of the state suggests that the  $6^+$  population decays to the postulated  $7^+$  level and then to the  $8^+$  isomer. The highly favored  $M1$  transitions within the multiplet thus channel strength into the  $8^+$  state in spite of  $E1$  competition to the lowest two states.

The hindrance factors of the  $E1$  transitions may be estimated crudely from the observed branching ratios and an estimate for the  $M1$  strengths between members of the  $(g_{9/2})^2$  multiplet. The reduced  $M1$  strengths<sup>31</sup> for the coupled neutron-proton system can be expressed as

$$B(M1, J_i \rightarrow J_f) = \frac{3}{4\pi} \begin{pmatrix} j & 1 & j \\ -j & 0 & j \end{pmatrix}^{-2} \begin{Bmatrix} J & J_f & j \\ J_i & j & 1 \end{Bmatrix}^2 \\ \times (2J_f + 1)(\mu_n - \mu_p)^2,$$

in which  $j$  is the angular momentum ( $\frac{9}{2}$  in this case) of the neutron or proton. The large parentheses and brackets are the  $3-j$  and  $6-j$  symbols.<sup>32</sup> If the magnetic moments of the neutron hole and proton are taken<sup>33</sup> from the nearby nuclei  $^{87}\text{Sr}$  and  $^{93}\text{Nb}$  and the resulting transition rates expressed in Weisskopf units,<sup>34</sup> we find for the transition  $3^+ \rightarrow 4^+$ , 4.1;  $4^+ \rightarrow 5^+$ , 3.6;  $5^+ \rightarrow 6^+$ , 3.0; and  $6^+ \rightarrow 7^+$ , 2.4. The hindrance factors of the competing  $E1$  decays relative to the Weisskopf single-particle estimate and then found to be 2600 for the  $4^+ \rightarrow 4^-$  decay and 7200 for the  $5^+ \rightarrow 5^-$ . Using the 1285-keV/298-keV intensity ratio from Ref. 9, the hindrance for the  $3^+ \rightarrow 4^-$  transition is 5000. From the upper limits of 5 mb for the  $6^+ \rightarrow 5^-$  decay and 15 keV for the  $6^+ \rightarrow 7^+$  separation, the lower limit of the  $6^+ \rightarrow 5^-$  hindrance would be  $2 \times 10^7$ , if internal conversion were neglected. In the region 10–15 keV the  $L1$ -shell internal-conversion coefficient<sup>35</sup> dominates, and is of the order of a factor of 10; then the  $6^+ \rightarrow 5^-$   $E1$  hindrance would be of the order of  $10^6$ . These hindrances are in the range typical of  $E1$  transitions in medium and

TABLE IV. Comparison of observed population cross sections (in mb) for the four lowest levels with the observed  $\gamma$  feeding from higher states and calculated direct neutron feeding.

$E_x$ (keV)	$J^\pi$	Observed $\gamma$ feeding	Calculated $n$ feeding	Total feeding	Observed population
0	$4^-$	582	253	835	975 <sup>a</sup>
232	$5^-$	147	181	328	403
393	$1^+$	50	74	124	114
674	$8^+$	0	37	200 <sup>b</sup>	136

<sup>a</sup> Average of measured  $^{89}\text{Y}(n, 2n)^{88}\text{Y}$  cross sections from Refs. 13, 26, and 27.

<sup>b</sup> Includes assumed unobserved feeding from  $7^+$  level; see text, Sec. IV.

heavy nuclei.<sup>36</sup>

The cross sections for the strong transitions can be accounted for reasonably well from the observed branching ratios and the calculated neutron feeding from selection II in Table III. These results are discussed below and summarized in Table IV. For the  $5^-$  (232-keV) level, the measured 147-mb  $\gamma$  feeding plus calculated 181-mb neutron population is 328 mb, which is to be compared with the observed decay of 403 mb. Most of the difference may be accounted for by the 53 mb of the probable 897-keV decay of the 1129-keV level. For the  $1^+$  (393 keV), the measured feeding of 50 mb plus calculated direct population of 74 mb is 124 mb; the observed decay is 114 mb. No  $\gamma$  rays feeding the  $8^+$  level directly are observed, and the calculated 37 mb is much too small to account for the 136-mb population of this isomer. Adding the calculated 54 mb of the  $7^+$  level yields 91 mb, which is still too small; it is necessary to include feeding from the  $6^+$  level as described above. Adding in the calculated 75 mb for direct population of the  $6^+$  and the observed 34 mb of  $\gamma$  rays feeding the  $6^+$  gives a total of 200 mb, which is larger than our value, but smaller than that observed in Ref. 13 with 14.8-MeV neutrons. This result may be due to the neglect of higher levels in  $^{89}\text{Y}$ ; the calculated values from selection I yield a total of 178 mb. Adding further levels in the region above 1500 keV may be expected to further improve the agreement by removing portions of the direct population of the  $6^+$ ,  $7^+$ , and  $8^+$  states to higher levels which can decay by bypassing the  $g_{9/2}^2$  multiplet. Throughout this calculation, the 706-keV level was assigned  $1^+$ . Assignments<sup>9</sup> of  $2^-$  would slightly increase the neutron feeding of this level, but not otherwise strongly affect the results.

We have attempted to show that in the present

case it is essential to include the detailed nuclear structure of the levels in the final nucleus to determine the isomeric cross sections. Since the  $Q$  values for the  $(n, 2n)$  reaction are in the range  $-10$  to  $-12$  MeV in many nuclei, the inability to use a statistical distribution of states in calculating the  $\gamma$  cascade to isomeric states following such reactions may be widespread. Even in those cases when a statistical description is appropriate for high excitation energies in the

final nucleus, the influence of special configurations at low energy can ordinarily not be calculated *a priori*. This question can be dealt with satisfactorily only if the low-lying states and their decay properties can be observed experimentally.

We are grateful to Dr. Helmut Baer and Dr. Joseph Comfort, who were associated with the Colorado and Argonne experiments, respectively, for sending us their results prior to publication.

<sup>†</sup>Work performed under the auspices of the U. S. Atomic Energy Commission.

\*Present address: General Electric Company, Vallecitos Nuclear Center, Sunol, California.

<sup>1</sup>C. D. Goodman, T. A. Hughes, M. W. Johns, and K. Way, Nucl. Data A8, 345 (1970).

<sup>2</sup>E. K. Hyde, M. G. Florence, and A. E. Larsh, Phys. Rev. 97, 1255 (1955).

<sup>3</sup>Leipunskii, Morozov, Makarov, and Yampol'skii, Z. Eksp. Teor. Fiz. SSSR 32, 393 (1957) [transl.: Sov. Phys. — JETP 5, 305 (1957)].

<sup>4</sup>A. M. Morozov and V. V. Remaev, Z. Eksp. Teor. Fiz. SSSR 43, 438 (1962) [transl.: Sov. Phys. — JETP 16, 314 (1963)].

<sup>5</sup>E. A. Ivanov, Rev. Roum. Phys. 12, 885 (1967).

<sup>6</sup>J. R. Comfort and J. P. Schiffer, Phys. Rev. C 4, 803 (1971).

<sup>7</sup>R. C. Bearse *et al.*, Phys. Rev. Lett. 23, 864 (1969).

<sup>8</sup>H. W. Baer, R. L. Bunting, J. E. Glenn, and J. J. Kraushaar, Nucl. Phys. (to be published).

<sup>9</sup>F. Gabbard, G. Chenevert, and K. K. Sekharan, Phys. Rev. C 6, 2167 (1972).

<sup>10</sup>Obtained from International Atomic Energy Agency, Vienna; Uncertainties  $\leq 1.3\%$ .

<sup>11</sup>E. Storm and H. Israel, Nucl. Data A7, 565 (1970).

<sup>12</sup>E. Monnard, Centre d'Etudes Nucleaires de Grenoble Report No. CEA-R2900, 1965 (unpublished).

<sup>13</sup>G. N. Salaita and P. K. Eapen, Trans. Am. Nucl. Soc. 16, 59 (1973).

<sup>14</sup>V. L. Glagolev and P. A. Yampol'skii, Z. Eksp. Teor. Fiz. SSSR 40, 743 (1961) [transl.: Sov. Phys. — JETP 13, 520 (1961)].

<sup>15</sup>L. Van Zelst, P. Meyers, and J. A. Oosting, Physica 39, 463 (1968).

<sup>16</sup>K. G. Broadhead, D. E. Shanks, and H. H. Heady, Phys. Rev. 139, B1525 (1965).

<sup>17</sup>P. S. Buchanan, S. C. Mathur, W. E. Tucker, I. L. Morgan, and E. L. Hudspeth, Phys. Rev. 158, 1041 (1967).

<sup>18</sup>J. B. Marion, Nucl. Data A4, 301 (1968).

<sup>19</sup>G. C. Dutt and F. Gabbard, Phys. Rev. 178, 1770 (1969).

<sup>20</sup>W. W. Daehnick and T. S. Bhatia, Phys. Rev. C 7, 2366 (1973).

<sup>21</sup>E. Vogt, in *Advances in Nuclear Physics* (Plenum, New York, 1968), Vol. 1, p. 261.

<sup>22</sup>F. Bjorklund and S. Fernbach, Phys. Rev. 109, 1295 (1958).

<sup>23</sup>S. M. Grimes, private communication.

<sup>24</sup>P. A. Moldauer, Nucl. Phys. 47, 65 (1963).

<sup>25</sup>J. J. Griffin, Phys. Rev. Lett. 17, 478 (1966).

<sup>26</sup>J. Károlyi, J. Csikai, and G. Pető, Nucl. Phys. A122, 234 (1968).

<sup>27</sup>R. Rieder and H. Münzer, Acta Phys. Austr. 23, 42 (1966).

<sup>28</sup>J. R. Huizenga, in *Statistical Properties of Nuclei*, edited by J. B. Garg (Plenum, New York, 1972), p. 438.

<sup>29</sup>J. R. Huizenga and R. Vandenbosch, Phys. Rev. 120, 1305 (1960).

<sup>30</sup>R. Vandenbosch and J. R. Huizenga, Phys. Rev. 120, 1313 (1960).

<sup>31</sup>M. A. Preston, *Physics of the Nucleus* (Addison-Wesley, New York, 1962), p. 299.

<sup>32</sup>A. R. Edmonds, *Angular Momentum in Quantum Mechanics* (Princeton U. P., Princeton, 1957).

<sup>33</sup>C. M. Lederer, J. M. Hollander, and I. Perlman, *Table of Isotopes* (Wiley, New York, 1967), 6th ed.

<sup>34</sup>D. H. Wilkinson, in *Nuclear Spectroscopy*, edited by F. Ajzenberg-Selove, (Academic, New York, 1960), Part B, p. 859.

<sup>35</sup>R. S. Hager and E. C. Seltzer, Nucl. Data A4, 1 (1968).

<sup>36</sup>C. F. Perdrisat, Rev. Mod. Phys. 38, 41 (1966).